Drought is a recurring challenge in the Middle East

David Kaniewski[a,b,1], Elise Van Campo[a,b], and Harvey Weiss[c]

[a]Laboratoire Ecologie Fonctionnelle et Environnement, Institut National Polytechique, Université Paul Sabatier, Université de Toulouse, 31062 Toulouse, France; [b]Laboratoire Ecologie Fonctionnelle et Environnement, Centre National de la Recherche Scientifique, 31062 Toulouse, France; and [c]Tell Leilan Project and School of Forestry and Environmental Studies, Yale University, New Haven, CT 06511

Edited by Ofer Bar-Yosef, Harvard University, Cambridge, MA, and approved February 1, 2012 (received for review October 5, 2011)

Climate change and water availability in the Middle East are important in understanding human adaptive capacities in the face of long-term environmental changes. The key role of water availability for sedentary and nomad populations in these arid to semiarid landscapes is understood, but the millennium-scale influence of hydrologic instability on vegetation dynamics, human occupation, and historic land use are unknown, which has led to a stochastic view of population responses and adaptive capacities to precipitation anomalies. Within the time-frame of the last two global climate events, the Medieval Climate Anomaly and the Little Ice Age, we report hydrologic instability reconstructed from pollen-derived climate proxies recovered near Tell Leilan, at the Wadi Jarrah in the Khabur Plains of northeastern Syria, at the heart of ancient northern Mesopotamia. By coupling climate proxies with archaeological-historical data and a pollen-based record of agriculture, this integrative study suggests that variability in precipitation is a key factor on crop yields, productivity, and economic systems. It may also have been one of the main parameters controlling human settlement and population migrations at the century to millennial timescales in the arid to semiarid areas of the Middle East. An abrupt shift to drier conditions at ca. AD 1400 is contemporaneous with a change from sedentary village life to regional desertion and nomadization (sheep/camel pastoralists) during the preindustrial era in formerly Ottoman realms, and thereby adds climate change to the multiple causes for Ottoman Empire "decline."

The historical region of Northern Mesopotamia was recently subjected to an intense and prolonged drought episode during the four hydrological years between AD 2007 and 2010. Very low precipitation generated a steep decline in agricultural productivity in the rain-fed Euphrates and Tigris drainage basins, and displaced hundreds of thousands of people (1). The worst drought-affected regions were eastern Syria, northern Iraq, and Iran, the major grain-growing areas of the northern Fertile Crescent. This episode corresponds to the driest 4-y period for the Fertile Crescent since AD 1940, just slightly drier than the AD 1998–2000 event (1), and is predicted to become more common as warming proceeds (2). Socioeconomic after-effects of this recent drought clearly challenge the common belief that agricultural societies, by technological innovation and societal adjustment, adaptively protect themselves from variability in natural precipitation (3). The large arid and semiarid zones of the Middle East rely on fragile systems of rain-fed or irrigated cultivation and are especially vulnerable to periodic fluctuations in climate and, most of all, to changes in hydrology. Anticipated repetitive drought episodes may exacerbate the vulnerability of communities unprepared to mitigate their adverse effects (4). During the last 40 y, many eastern dryland countries (Iran, inland Israel, Jordan, Turkey) have experienced warming and precipitation decline (5–8). Drought periods have recurred in an irregular and nonuniform manner, with highest severity, magnitude, and duration over the last decade (7). Interacting with other social, economic, and political variables, they act as a "threat multiplier" (4, 9). The Middle East has long since exceeded the water resources necessary to supply its population, and has sought to expand water distribution and storage systems through dams and canals until droughts and falling water supplies in aquifers became critical. Throughout the recent crisis and its aftermath (1), eastern Syria reveals the same environmental vulnerability as in antiquity that may severely impact farming constituencies (4).

The critical role of water availability in ancient Mesopotamia is well-documented in archaeological and historical records (10, 11). In Northern Mesopotamia, the end of the Late Uruk colony period at ca. 5.2 kyr BP and the desertion of the Akkadian imperialized landscape at ca. 4.2 kyr BP (12) have fueled debate on the complex interactions between hydrologic instability, human adaptation/migration, and urban origin/decline (13–15). Thresholds above which agro-innovations were not achievable led to regional habitat-tracking to riparian, paludal, and karst spring-fed refugia (16). The 5.2 and 4.2 kyr BP arid events are widely recorded in Mediterranean and Southwest Asian paleoclimatic records (17–21). Independent archaeological and paleoclimate data suggest a causal link between low precipitation-higher dust input, decline of rain-fed agriculture (beyond sustainable limits), and population desertion that may lead to adaptive regional abandonment and nomadization. On the Khabur Plains of northeastern Syria (the northern Jazira), rain-fed (> 250 mm/y^{-1}) agriculture has been practiced since the earliest domestication of plants (22). Access to reliable and permanent water/groundwater resources was the key ecological constraint to cultivation and settlement then, and is still the case throughout much of the Middle East and worldwide in semiarid to arid zones (23).

The last millennium contained two contrasted climatic periods of widespread temperature and hydrological anomalies: the Medieval Climate Anomaly (MCA) and the Little Ice Age (LIA), from approximately AD 900–1300 and AD 1550–1850, respectively (24). This article investigates the hydrologic instability in the Khabur Plains-northeastern Syria (Fig. 1), at the heart of ancient northern Mesopotamia during these two periods. Pollen-derived information on vegetation changes were used to reconstruct hydrological trends and assess the role of hydrologic instability in human occupation and agricultural production at the millennial/centennial scale. The modern consequences of the current AD 2007–2010 drought event resonate with the historical association of precipitation variation with population migration and desertion in northern Mesopotamia.

Modern Climatic Setting

At the eastern end of the Mediterranean basin, the climate of the Khabur Plains exhibits hot dry summers and cool wet winters. Most of the cold-season precipitation is a result of midlatitude troughs that propagate from the North Atlantic Ocean and reactivate over the Eastern Mediterranean sea (25). The Khabur Plains are characterized by steep rainfall gradient and high interannual climate variability. North of the plain, rainfall amounts reach ca. 500 mm/y^{-1} (26), whereas southwards, at Al Hassakah (36°29′40.46′′N; 40°46′05.88′′E; 313 m above sea level), mean annual precipitation (MAP) and temperature are about 290 mm/y^{-1} and 18 °C, respectively. The rainy season extends from

Author contributions: D.K., E.V.C., and H.W. designed research, performed research, analyzed data, and wrote the paper.

The authors declare no conflict of interest.

This article is a PNAS Direct Submission.

[1]To whom correspondence should be addressed. E-mail: david.kaniewski@univ-tlse3.fr.

This article contains supporting information online at www.pnas.org/lookup/suppl/doi:10.1073/pnas.1116304109/-/DCSupplemental.

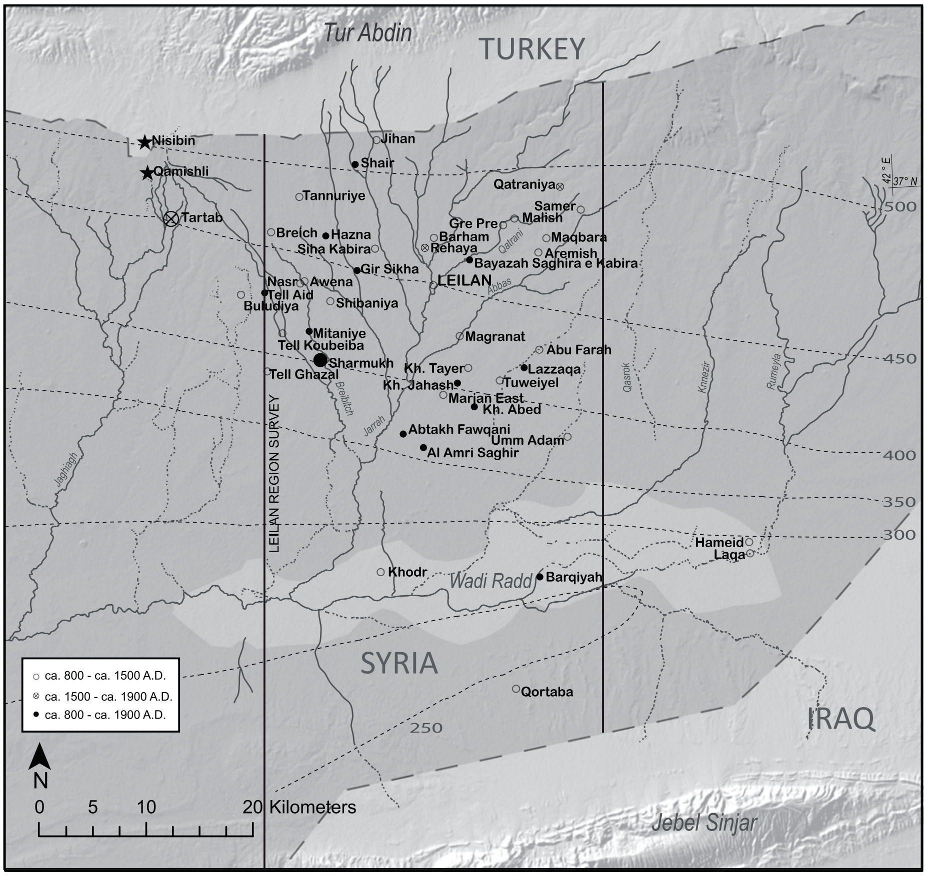

Fig. 1. Map of northeastern Syria with an overview of Wadi Jarrah in the Khabur Plains, northern Jazira. Period-wise village level settlement (<4 ha) indicated with small circles; likely larger settlements are Tartab (partial destruction by modern road-construction, 1985) and multisite Charmoukh (probably ancient capital city Adhrama). Precipitation isohyets are mm/annum.

December to April (80% of MAP), whereas rainfall in June, July, and August accounts for only 0.2% of the annual total. The Khabur River, the southernmost major tributary of the Euphrates system (27), rises in Southern Anatolia, and grows substantially from the input of major karstic springs after crossing the Turkey-Syria border (28). The Wadi Jaghjagh and the Wadi Jarrah systems (Fig. 1) are rainfall-dependent and fed by the effluents emanating from the Tur Abdin Mountains, north of the Khabur Plains.

Results and Discussion

Dry vs. Wet Steppe Landscapes. The Wadi Jarrah region is now a semiarid steppe characterized by low annual precipitation and strong wind erosion, as is the entire Khabur Plains (29). It lies in the steppe vegetation class of *Artemisietea herbae–albae mesopotamica*, which includes dwarf-shrub or herbaceous formations of the Irano-Turanian territories (30). The vegetation has been overgrazed and deprived of its shrubby constituents by climate and human pressures (30), as shown by low arboreal pollen percentages throughout the last millennium (19–43%), with a submodern value less than 25% of the terrestrial pollen sum. Warm mixed woodland [WMW; (e.g., deciduous *Quercus*, *Fraxinus*, *Pinus*, *Platanus*)] and xeric wood/shrub [XWS; (e.g., *Crataegus*, *Juniperus*, *Pistacia*)] (Fig. 2) tend to disappear during the AD 20th century (Fig. 3).

The two main pollen-derived vegetation patterns (PdV) (Fig. 2) isolated for the last 1,600 y, dry shrub-steppe (DSS) and moist forb-grass meadow steppe (MGS), correspond to two contrasted components of steppic environment (Fig. 3). These two time-series are significantly anticorrelated with the highest correlation coefficient centered on Lag_0 (−0.95, $P = 0.05$) (Fig. 4). The arid component [−0.72 of total variance on principal components analysis (PCA)-Axis 1] is led by forbs (nonwoody plants other than grass, sedge, rush; for example, *Artemisia herba-alba*, Asteraceae, Chenopodiaceae/Amaranthaceae, *Ephedra*) mixed with xeric shrubs (e.g., *Tamarix*, *Teucrium*, *Ziziphus*). The development of a permanent DSS at Wadi Jarrah, the equivalent of the modern *Artemisietea herbae–albae mesopotamica* steppe, has occurred since ca. AD 1400 (Fig. 3). Previous increases were recorded before AD 500 and at ca. AD 800 (Fig. 3).

The PdV DSS (Fig. 2) is similar to modern pollen-based vegetation recorded in the Iranian desert-steppe (31), at Ramlat as-Sab'atayn in Yemen (32), at Abu-Madi on the Nile Delta (33), at low elevation in Central Jordan (34), and on the Alashan Plateau (35) in China. This Asian/Arabian semiarid desert/steppic environment is mainly driven by climate (low rainfall, wind erosion) and instable/poor soil (sandy/rocky type). Similar vegetation patterns were recorded during parts of the Early and Late Holocene at Wadi Dana, Jordan (36), and at Khawr Rawri and Khawr Al Balid, Sultanate of Oman (37). The DSS is linked in the neighbor joining clustering (NJ) with XWS (Fig. 4), although a part of the tree pollen-types from this cluster (Fig. 2) may result from long-distance transport from northern mountains.

The PdV MGS wet component (+0.67 of total variance on PCA-Axis 1) is loaded by grass (Poaceae) and hygrophytes (e.g., Cyperaceae, Ranunculaceae, *Typha*/*Sparganium*) with meadow forbs (e.g., Apiaceae, Caryophyllaceae, Malvaceae, Primulaceae, Rubiaceae). The MGS is dominant in the surroundings of the river channel at ca. AD 530–750 and ca. AD 850–1350. A large peak is last recorded at ca. AD 1750. The PdV MGS is similar to marsh areas recorded during the Early Holocene in the north-eastern Rub' al-Khali desert, Arabian Peninsula (38), and in the modern pollen-based vegetation at Baltim, Nile Delta-Egypt (33), at Gravgaz, Turkey (39), at Cherepan and Trialeti, Caucasus (40), and in Qaidam basin, China (41). The MGS is linked in the NJ with the WMW (Fig. 2), suggesting a close link with the modern vegetation patterns at Cherepan and Trialeti near Tbilisi (40), defined by a MAP of 495.5 mm/y^{-1}. The expansion of a wet steppe/forest-steppe is often correlated with humid conditions at

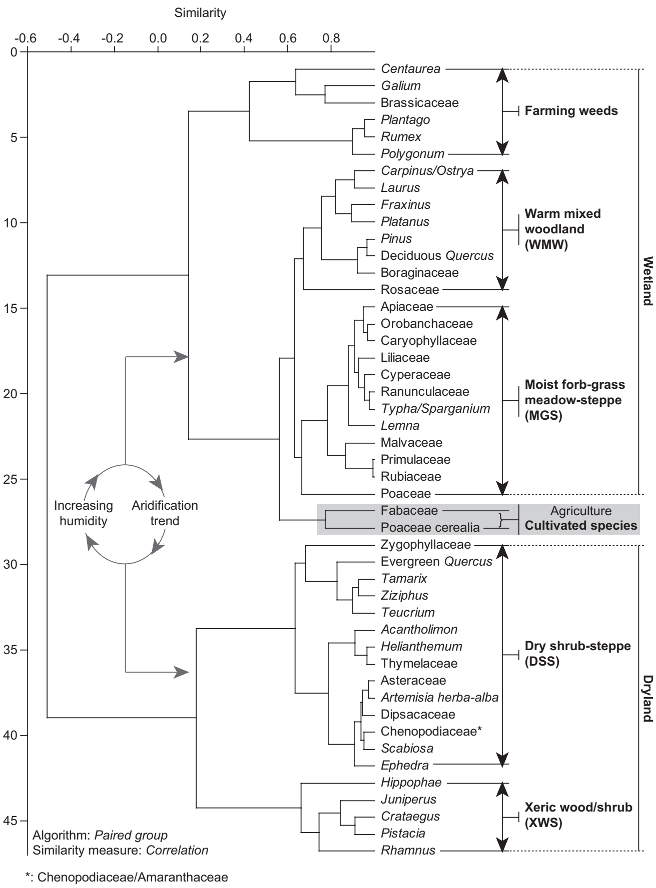

Fig. 2. Cluster analysis of the main taxa from Wadi Jarrah and suggested pollen-derived vegetation patterns.

all these sites. The development of swampy forbs in and around the river channel and the growth of a wet meadow steppe at Wadi Jarrah are directly linked with higher input of freshwater and increased water availability in soils, generated by higher rainfall and gravity flow on the alluvial plain.

DSS and MGS PdV (dry vs. wet) correspond to the main loadings in the PCA, explaining most of the variance for the PCA-Axis 1 ordination of the data, which accounts for +0.939 of total inertia (Fig. 3). Arid DSS (−0.72) and XWS (−0.03) are loaded in negative values, whereas positive values correspond to wet MGS (+0.67) and WMW (+0.16). DSS and MGS also constitute the two distant branches in the NJ (Fig. 4), and samples in the kernel-density map are clearly split by these two components (Fig. 4). Variations in PCA-Axis 1 values therefore reflect changes in water availability through the MCA and LIA periods.

Development of Sedentary Life. During antiquity and Islamic times, the Khabur Plains were crossed by the Euphrates trade route (‘Abbāsid Road) connecting Aleppo to Mosul through the northern Mesopotamian plateau, and formed an important link between western Syria and northern Mesopotamia (42). Along Wadi Jarrah, the Tell Leilan Region surface survey and historical data both document Early Islamic, ‘Abbāsid, Ayyūbid, Mamluk, and Ottoman settlement patterns with considerable variability (43).

The period encompassing the MCA corresponds to a gradual enlargement of surveyed settlements in the region of Tell Leilan during the ‘Abbāsid period (AD 10–11th centuries), reaching a height of occupation during the Ayyūbid dynasty (AD 12–13th centuries, 30 settlements) and Mamluk sultanate (AD end 13th–14th centuries, 20 settlements) (Fig. 3). This period corresponds to a main positive deviation on the PCA-Axis 1 at ca. AD 850–1350, suggesting overall higher water input in the area, although short-term drought events are mentioned in the Chronicle of Michael the Syrian (44). High scores in the warm/cool steppe (WAST/COST) ratio (ca. AD 1050–1300), are indicative of a warming trend. Agricultural activities (Fig. 3), led by Poaceae cerealia (e.g., barley, wheat) and Fabaceae (e.g., fava bean, *Pisum* sp., *Cicer* sp., *Lens culinaris*), reach a peak at ca. AD 1100–1350, with farming weeds/secondary anthropogenic indicators (e.g., *Centaurea*, *Plantago*, *Rumex*, *Polygonum*). According to medieval geographers (e.g., ibn Šaddād, AD 13th century), a time of political safety and agro-economic development extended from the Ayyūbid dynasty to the Mamluk sultanate, despite the presence of threatening pastoralist tribal groups (45). The text of ibn Šaddād provides a list of regional products for the northern Jazira, including wheat, barley, rice, and sesame. Wheat (above MAP 300 mm/y^{-1}) and barley (MAP 200–300 mm/y^{-1}) were cultivated during the MCA and are still the most important cereal crops in the semiarid Eastern Mediterranean region (46). Today, irrigated agriculture essentially develops along the major floodplains of the Euphrates or is confined to areas with permanent groundwater (47). The region’s traditional agriculture, characterized by rain-fed cultivation and gravity-flow irrigation, is mainly concentrated on wheat and barley (48, 49), the latter because of its high resistance to salinity and tolerance of poor soils (50). Nonirrigated crops, particularly sensitive to precipitation variability that may affect the area, are becoming a key factor in crop yields, productivity, and economic systems (1). Favored by wet-warm conditions and an active river channel, agro-productivity reached a maximum during the MCA, leading to sedentary life and the development of an extended town/village agro-economy.

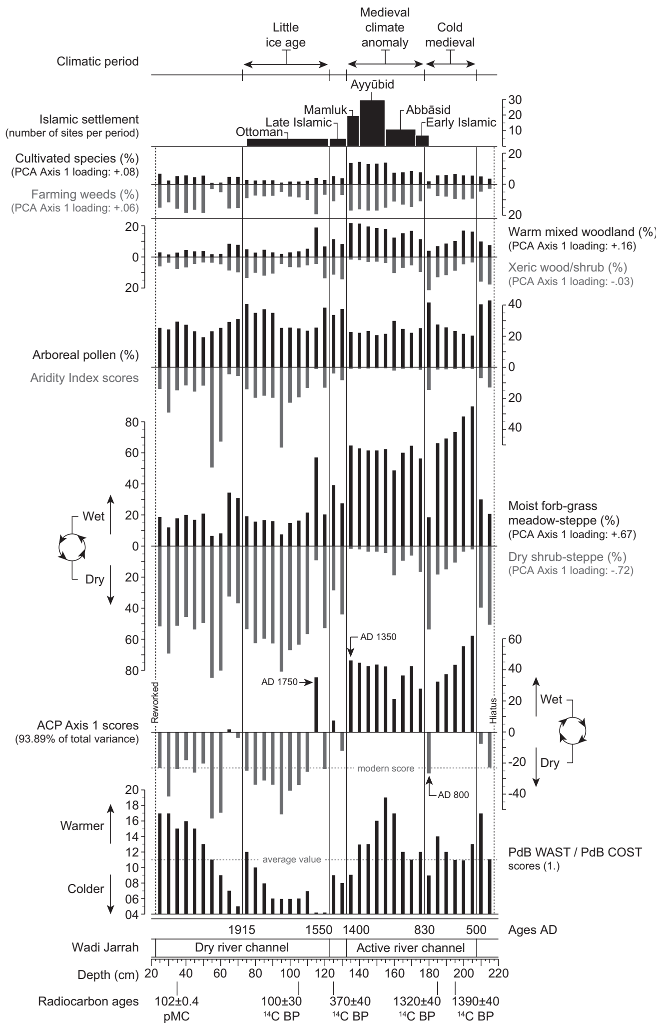

Fig. 3. The last 1,600 y from the viewpoint of pollen-derived climatology. The pollen-derived proxy of moisture availability is drawn as PCA-Axis 1 scores. Temperature changes are reported by the warm-cool ratio WAST/COST. The pollen-derived vegetation patterns and the cultivated species are shown on a linear depth-scale. The main climatic events, and the historical-cultural periods (with the number of settlements) are indicated at the top of the diagram.

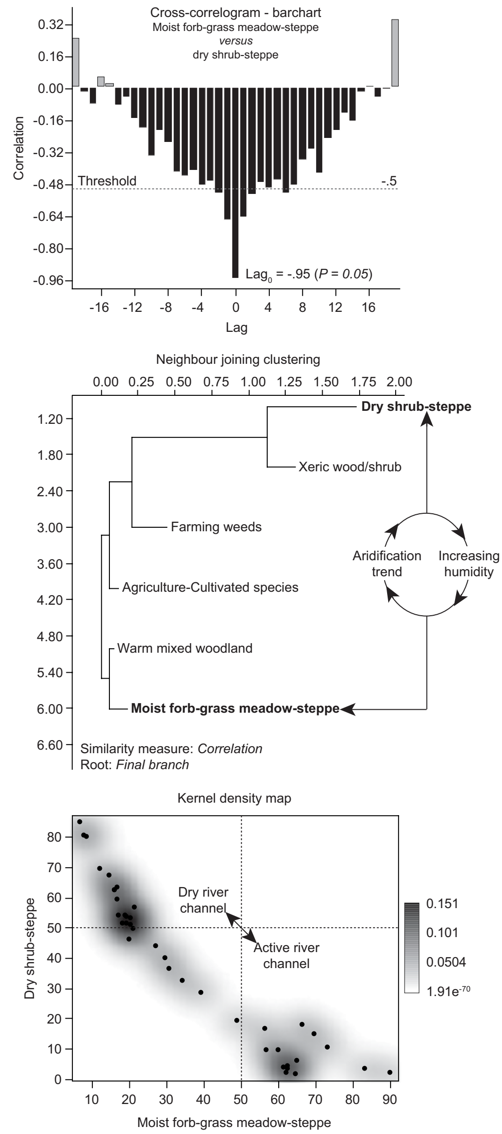

Fig. 4. Cross-correlogram ($P = 0.05$) DSS vs. MGS, NJ analysis (with "correlation" as similarity measure and "final branch" as root), and kernel-density map (bootstrap 100 × 100) DSS vs. MGS.

The positive rainfall anomalies recorded in northern Jazira (Fig. 3) are correlated with humid conditions in southern Levant as reported by the $\delta^{18}O$ records from Soreq Cave (51) and the Ashdod coast (52, 53), both showing minimal $\delta^{18}O$ values between ca. AD 1050 and 1350 [termed "Event II" (53)]. Increases in winter precipitation amounts at Nar Gölü (54), low $\delta^{18}O$ values in the Red Sea (55), enhanced Nile floods (56), higher fluvial inputs in the Arabian Sea off Pakistan (57), stronger Indian monsoon (58), and high water levels in the Saharan Lakes (59) show that wetter climatic conditions prevailed throughout the Middle East and in the nearby tropical zones during the time period coinciding with the MCA. Warm and wet MCA in the Middle East contrasts with the modern warm and dry conditions, and the predictions of climate models, which clearly show that warming would lead to drier bio-climatic conditions (5). The relationship between changes in temperature and precipitation appear quite complex. During the following intermediate phase (AD 1400–1550) and the LIA, a drier and cooler climate developed in the region. Dry conditions still prevail today, but with warmer temperatures (Fig. 3).

Abandonment of Sedentary Life. This settlement pattern changed after the 14th century AD, at the end of the Mamluk sultanate. A significant drop in the number of occupied sites indicates heavy depopulation during the Late Islamic (AD 15–16th centuries) and Ottoman (AD 17th to the beginning of the 20th century) periods (43, 48, 60–62). By the late 1500s, the core Mediterranean lands of the Ottoman Empire (Greece, southern Bulgaria, Anatolia, Syria, and Palestine) suffered from the increased warfare (63) and previous demographic growth had strongly eroded the ecological capacity of the territories. Because most of the peasants were overwhelmingly dependent on a single crop of winter wheat or barley, semiarid farmland left them exposed to climate fluctuations. At Wadi Jarrah, the end of sedentary agricultural village settlement and regional abandonment are coincident with lower cultivation from AD 1400 onward, and also with the high development of DSS and drought-driven major hydrological changes. Most negative scores in the PCA-Axis 1 are recorded between ca. AD 1550 and 1960, after an isolated peak at ca. AD 1400 (Fig. 3). The lowest temperatures, as suggested by the lowest scores of the WAST/COST ratio, were recorded during the LIA (Fig. 3). The area became drier and

ENVIRONMENTAL SCIENCES

Table 1. Details of the AMS ^{14}C age determinations for the Wadi Jarrah core

Code	Material	AMS ^{14}C yr BP	Δ13C (‰)	Calibrated dates AD 1σ–68%	Calibrated dates AD 2σ–95%
β-281565	Seeds	102 ± 0.4 pMC	−25.3	Post-1950	
β-281556	Seeds	100 ± 30	−24.1	1815–1840/1865–1895	1805–1935
β-281566	Seeds	370 ± 40	−24.3	1455–1520	1445–1530
β-281557	Seeds	1,320 ± 40	−28.5	655–695	650–775
β-281567	Seeds	1,390 ± 40	−23.9	620–665	575–690

cooler. Precipitation and groundwater were probably insufficient to maintain sustainable agriculture. Tribal pastoralists may have taken advantage of the abandonment of the drying river alluviums to intensify their raids, accelerating the end of agricultural settlement at abandoned village loci (48). Around Tell Leilan, rare but significant Islamic artifacts, unglazed pottery production, and clay pipe fragments, document nomadic occupations of the area at this time, probably by sheep and camel herders. These nomadic settlements and regional abandonments are recorded at several places on the Khabur Plains, and adjacent northern Iraq during the LIA (43). The climate change adds an important factor within long-standing debates about the nature of the late Ottoman agro-political economy (64).

The changing hydrologic conditions, leading to a dry LIA in northern Mesopotamia, are also indicated by marked increases in $\delta^{18}O$ values on Ashdod coast (52, 53), Soreq Cave (51), and Nar Gölü (54). Decreased precipitation in Central Asia (65), weaker Indian monsoon (58), reduced Nile floods (56), and extreme dry events in the north Aegean (66) corroborate the hydrologic instability and the extended drought during the LIA.

Submodern Conditions. Although largely uninhabited during the AD 19th century, tribal Arab and Kurdish pastoralists and agriculturalists have repopulated the Khabur Plains since the onset of the AD 20th century, and continuing with the development of several small cities, hundreds of villages and hamlets since AD 1930–1940 (60, 67). Climate proxies (Fig. 3) show that the important submodern resettlements (AD 20th century) occurred after the last dry peaks around ca. AD 1925–1930. A first peak of resettlement was probably reached just after the first World War, with market driven and railroad-facilitated wheat cropping on the extensive unsettled Khabur Plains (68, 69). The full resettlement of the Khabur Plains corresponds with an expansion of agriculture in the wettest northern zones and the extension of dry farming onto the steppe. The latter event was achieved by pump irrigation, which has led to summer aridification of rivers, strong wind erosion, and soil salinization, forcing a decline in water table and water quality. Despite the adaptive capacities led by impressive agro-innovations during the AD 20th century, populations in northern Jazira are still vulnerable and cannot adapt in place to environmental changes, such as the recent AD 2007–2010 drought event.

Materials and Methods

Lithology and Chronology. The Wadi Jarrah (36°51′51.52′′N; 41°14′15.15′′E; 374 m above sea level) is today a dry river channel of the Khabur Plains, located 20 km south of the Turkish border and 40 km north of the Iraqi border (Fig. 1). The 210-cm sedimentary deposits of the Wadi Jarrah (Fig. S1) consist of dark, sandy silts with gravels in the upper section, and muddy clay with zones of abundant gastropod and pelecypod shells (still fully articulated) in the lower section. These sedimentary deposits are the result of a shift from a meandering to braided river channel system, completely dry today, and indicate regional changes in hydrology. The chronology is based on five accelerator mass spectrometry (AMS) radiocarbon (^{14}C) ages (Table 1), performed on scarce plant remains. The AMS ^{14}C dates show an orderly relationship with depth and are therefore considered reliable. All conventional radiocarbon ages have been calibrated (one- and two-σ calendar calibration) using Calib-Rev. 6.0.1 (70) and Oxcal 4.1 (71).

Pollen Analysis. A total of 40 samples were prepared for pollen analyses using standard palynological procedures. Pollen grains were counted under 400× and 1,000× magnification using an Olympus microscope. Pollen frequencies (%) are based on the total pollen sum (average: 525 pollen grains) excluding local hygrophytes and spores of nonvascular cryptogams. Aquatic taxa frequencies are calculated by adding local hygrophytes-hydrophytes to the terrestrial pollen sum. The arboreal pollen curve, calculated by summing frequencies of arboreal taxa for each sample, provides an estimate of the relative forest density.

Numerical Analyses. Paucity of regional modern pollen spectra prevent a pollen-based quantification of changes in temperature and rainfall amount, which was approached by the following methods. Pollen data have been converted into PdV, using cluster analysis (algorithm: *paired group*; similarity measure: *correlation*) (Fig. 2). Pollen types from each cluster were summed to create PdV time-series with DSS, MGS, XWS, and WMW (Fig. 3). PCA was then performed to test the ordination of samples by assessing major changes in PdV-frequencies. The main variance is loaded by the PCA-Axis 1. PdV-frequencies and PCA-Axis 1 scores have been plotted on a linear depth-scale (Fig. 3). The modern score line drawn on the PCA-Axis 1 corresponds to the value of the upper sample (Fig. 3). An aridity index was computed by the ratio DSS vs. MGS PdV (Fig. 3). Pollen data have also been converted into plant functional types and a pollen-derived biomization of the plant functional types has been elaborated based on appropriate methods (72, 73). Pollen-derived biomes are similar to the regional studies in the Mediterranean and Kazakhstan (73), featuring WAST and COST. Temperature changes are elucidated using the warm-cool WAST/COST ratio (Fig. 3).

A linear detrended cross-correlation ($P = 0.05$) was then applied to assess the relationships between DSS vs. MGS time-series (Fig. 4). Positive/negative correlation coefficients are considered, focusing on the Lag_0 value (with +0.50/−0.50 as significant thresholds). The ecological distance DSS vs. MGS was further tested using NJ clustering (Fig. 4). NJ analysis (*correlation* as similarity measure and *final branch* as root) was used to compute the lengths of branches of a tree, using branches as ecological distances. A kernel-density map (bootstrap 100 × 100) was established to stress the distribution of samples according to DSS vs. MGS time-series (Fig. 4).

ACKNOWLEDGMENTS. The authors thank M. R. Besonen and M. Cremaschi for having undertaken the geoarchaeological sampling at Tell Leilan and Wadi Jarrah; the late Adnan Bounni and the Directorate-General of Antiquities and Museums, Damascus, for field research support; and E. Friedlander and T. Otto for technical assistance. This research was funded by the Mediterranean Integrated Studies at Regional And Local Scales (MISTRALS) PaléoMex-Centre National de la Recherche Scientifique programs and the Yale University Tell Leilan Project.

1. Trigo RM, Gouveia C, Barriopedro D (2010) The intense 2007–2009 drought in the Fertile Crescent: Impact and associated atmospheric circulation. *Agric For Meteorol* 150:1245–1257.
2. Chenoweth J, et al. (2011) Impact of climate change on the water resources of the eastern Mediterranean and Middle East region: Modeled 21st century changes and implications. *Water Resour Res* 47:W06506.
3. Lobell DB, et al. (2008) Prioritizing climate change adaptation needs for food security in 2030. *Science* 319:607–610.
4. Sowers J, Vengosh A, Weinthal E (2011) Climate change, water resources, and the politics of adaptation in the Middle East and North Africa. *Clim Change* 104:599–627.
5. Kafle HK, Bruins HJ (2009) Climatic trends in Israel 1970–2002: Warmer and increasing aridity inland. *Clim Change* 96(1–2):63–77.
6. Tayanç M, İm U, Doğruel M, Karaca M (2009) Climate change in Turkey for the last half century. *Clim Change* 94:483–502.
7. Al-Qinna MI, Hammouri NA, Obeidat MM, Ahmad FY (2011) Drought analysis in Jordan under current and future climates. *Clim Change* 106:421–440.

8. Soltani S, Saboohi R, Yaghmaei L (2012) Rainfall and rainy days trend in Iran. *Clim Change* 110(1–2):187–213.
9. Evans JP (2008) 21st century climate change in the Middle East. *Clim Change* 92: 417–432.
10. Postgate JN (1992) *Early Mesopotamia* (Routledge, New York).
11. Weiss H, et al. (1993) The genesis and collapse of third millennium north mesopotamian civilization. *Science* 261:995–1004.
12. Staubwasser M, Weiss H (2006) Holocene climate and cultural evolution in late prehistoric early historic West Asia. *Quat Res* 66:372–387.
13. deMenocal PB (2001) Cultural responses to climate change during the late Holocene. *Science* 292:667–673.
14. Weiss H, Bradley RS (2001) Archaeology. What drives societal collapse? *Science* 291: 609–610.
15. Lawler A (2010) Archaeology. Collapse? What collapse? Societal change revisited. *Science* 330:907–909.
16. Weiss H (2012) Altered trajectories: The Intermediate Bronze Age. *The Oxford Handbook of the Archaeology of the Levant*, eds Killebrew A, Steener M (Oxford Univ Press, Oxford).
17. Sirocko F, et al. (1993) Century-scale events in monsoonal climate over the past 24,000 yrs. *Nature* 364:322–324.
18. Bar-Matthews M, Ayalon A, Kaufman A (1997) Late quaternary paleoclimate in the eastern Mediterranean region from stable isotope analysis of speleothems at Soreq Cave, Israel. *Quat Res* 47(2):155–168.
19. Cullen HM, et al. (2000) Climate change and the collapse of the Akkadian empire: Evidence from the deep sea. *Geology* 28:379–382.
20. Arz HW, Lamy F, Pätzold J (2006) A pronounced dry event recorded around 4.2 ka in brine sediments from the northern Red Sea. *Quat Res* 66:432–441.
21. Parker AG, et al. (2006) A record of Holocene Climate Change from lake geochemical analyses in southeastern Arabia. *Quat Res* 66:465–476.
22. Bar-Yosef O (2011) Climatic fluctuations and early farming in West and East Asia. *Curr Anthropol* 52(4):175–193.
23. DePauw E, Gobel W, Adam H (2000) Agrometeorological aspects of agriculture and forestry in the arid zones. *Agric For Meteorol* 103(1–2):43–58.
24. Mann ME, et al. (2009) Global signatures and dynamical origins of the Little Ice Age and Medieval Climate Anomaly. *Science* 326:1256–1260.
25. Lionello P, Malanotte-Rizzoli P, Boscolo R (2006) *Mediterranean Climate Variability* (Elsevier, Amsterdam).
26. Weiss H (1986) The origins of Tell Leilan and the conquest of space in third millennium Mesopotamia. *The Origins of Cities in Dry Farming Syria and Mesopotamia in Third Millennium B.C.*, ed Weiss H (Four Quarters, Guilford, CT), pp 71–108.
27. Evans J, Geerken R (2004) Discrimination between climate and human-induced dryland degradation. *J Arid Environ* 57:535–554.
28. Burdon DJ, Safadi C (1963) Ras-el-Aïn: The great karst spring of Mesopotomia. A hydrogeological study. *J Hydrol (Amst)* 1(1):58–95.
29. Kerbe J (1987) *Climate, Hydrology and Hydro-Agricultural Development in Syria* (French) (Presses Universitaires de Bordeaux, Bordeaux).
30. Zohary M (1973) *Geobotanical Foundations of the Middle East* (G. Fischer, Stuttgart, Germany).
31. Wright HE, McAndrews JH, Van Zeist W (1967) Modern pollen rain in western Iran, and its relation to plant geography and Quaternary vegetational history. *J Ecol* 55: 415–443.
32. Lézine AM, Saliège JF, Robert C, Wertz F, Inizan ML (1998) Holocene lakes from Ramlat as-Sab'atayn (Yemen) illustrate the impact of Monsoon activity in Southern Arabia. *Quat Res* 50:290–299.
33. Ayyad SM, Moore PD, Zahran MA (1992) Modern pollen rain studies of the Nile Delta, Egypt. *New Phytol* 121:663–675.
34. Davies CP, Fall PL (2001) Modern pollen precipitation from an elevational transect in central Jordan and its relationship to vegetation. *J Biogeogr* 28:1195–1210.
35. Herzschuh U, Kürschner H, Battarbee R, Holmes J (2006) Desert plant pollen production and a 160-year record of vegetation and climate change on the Alashan Plateau, NW China. *Vegetation History and Archaeobotany* 15(3):181–190.
36. Hunt CO, et al. (2004) Early Holocene environments in the Wadi Faynan, Jordan. *Holocene* 14:921–930.
37. Hoorn C, Cremaschi M (2004) Late Holocene palaeoenvironmental history of Khawr Rawri and Khawr Al Balid (Dhofar, Sultanate of Oman). *Palaeogeogr Palaeoclimatol Palaeoecol* 213(1–2):1–36.
38. Parker AG, et al. (2004) Holocene vegetation dynamics in the northeastern Rub' al-Khali desert, Arabian Peninsula: A phytolith, pollen and carbon isotope study. *J Quaternary Sci* 19:665–676.
39. Vermoere M, et al. (2002) Late Holocene local vegetation dynamics in the marsh of Gravgaz (southwest Turkey). *J Paleolimnol* 27:429–451.
40. Connor SE, et al. (2004) A survey of modern pollen and vegetation along an altitudinal transect in southern Georgia, Caucasus region. *Rev Palaeobot Palynol* 129: 229–250.
41. Chen H, et al. (2006) Surface pollen in the east of Qaidam Basin. *J Geogr Sci* 16: 439–446.
42. Fiey JM (1964) The Iraqi section of the Abbasid Road Mosul-Nisibin. *Iraq* 26(2): 107–117.
43. Vezzoli V (2008) Islamic period settlement in the Tell Leilan Region (Northern Jazira): The material evidence from the 1995 survey. *Levant* 40:185–202.
44. Widell M (2007) Historical evidence for climate instability and environmental catastrophes in Northern Syria and the Jazira: The Chronicle of Michael the Syrian. *Environ Hist* 13(1):47–70.
45. Eddé-Terrasse AM (1984) Description of northern Syria, annotated translation of Izz al-din ibn Saddad, al-a'laq al-Hatira fî dikr umara' al-sam wa l-Ğazira (French). (Institut Français d'Etudes Arabes de Damas, Damas).
46. Izzi G, Farahani HJ, Bruggeman A, Oweis TY (2008) In-season wheat root growth and soil water extraction in the Mediterranean environment of northern Syria. *Agric Water Manage* 95:259–270.
47. Beaumont P (1996) Agricultural and environmental changes in the Upper Euphrates catchment of Turkey and Syria and their political and economic implications. *Appl Geogr* 16(2):137–157.
48. Hütteroth W (1998) Northeastern Syria and adjoining parts of Iraq and Turkey under early Ottoman rule (16^{th} century). *ARAM* 9–10:357–363.
49. McCorriston J, Weisberg S (2002) Spatial and temporal variation in Mesopotamian agricultural practices in the Khabur basin, Syrian Jazira. *J Archaeol Sci* 29:485–498.
50. Jacobsen T, Adams RM (1958) Salt and silt in ancient Mesopotamian agriculture: Progressive changes in soil salinity and sedimentation contributed to the breakup of past civilizations. *Science* 128:1251–1258.
51. Bar-Matthews M, Ayalon A, Gilmour A, Matthews A, Hawkesworth CJ (2003) Sea-land oxygen isotopic relationships from planktonic foraminifera and speleothems in the Eastern Mediterranean region and their implication for paleorainfall during interglacial intervals. *Geochim Cosmochim Acta* 67:3181–3199.
52. Schilman B, Bar-Matthews M, Almogi-Labin A, Luz B (2001) Global climate instability reflected by Eastern Mediterranean marine records during the Late Holocene. *Palaeogeogr Palaeoclimatol Palaeoecol* 176(1–4):157–176.
53. Schilman B, Ayalon A, Bar-Matthews M, Kagan EJ, Almogi-Labin A (2002) Sea-Land paleoclimate correlation in the Eastern Mediterranean region during the Late Holocene. *Isr J Earth Sci* 51(3–4):181–190.
54. Jones MD, Roberts CN, Leng MJ, Türkeş M (2006) A high-resolution Late Holocene lake isotope from Turkey and links to North Atlantic and monsoon climate. *Geology* 34:361–364.
55. Lamy F, Arz HW, Bond GC, Bahr A, Pätzold J (2006) Multicentennial-scale hydrological changes in the Black Sea and northern Red Sea during the Holocene and the Arctic/North Atlantic Oscillation. *Paleoceanography* 21:PA10008, doi:10.1029/ 2005PA001184.
56. Hassan FA (2007) Extreme Nile floods and famines in Medieval Egypt (AD 930-1500) and their climatic implications. *Quat Int* 173–174:101–112.
57. Lückge A, Doose-Rolinski H, Khan AA, Schulz H, von Rad U (2001) Monsoonal variability in the northeastern Arabian Sea during the past 5000 years: Geochemical evidence from laminated sediments. *Palaeogeogr Palaeoclimatol Palaeoecol* 167: 273–286.
58. Gupta AK, Das M, Anderson DM (2005) Solar influence on the Indian summer monsoon during the Holocene. *Geophys Res Lett*, 10.1029/2005GL022685.
59. Williams MAJ, Faure H (1980) *The Sahara and the Nile* (Balkema, Rotterdam).
60. Wirth E (1964) The agricultural plains of northeast Syria (German). *Geogr Z* 52(1): 7–42.
61. Göyünc N, Hütteroth WD (1997) *Borderland: Ottoman Administration of the Modern Turkish-Syrian-Iraqi Border Region in the 16th Century (German)* (Eren, Istanbul).
62. Wilkinson TJ, Tucker DJ (1995) *Settlement Development in the North Jazira, Iraq.* (British School of Archaeology in Iraq, Warminster).
63. White S (2011) *The Climate of Rebellion in the Early Modern Ottoman Empire* (Cambridge Univ Press, Cambridge).
64. Faroqhi SN (2006) *The Cambridge History of Turkey* (Cambridge Univ Press, Cambridge).
65. Sorrel P, Popescu SM, Klotz S, Suc JP, Oberhänsli H (2007) Climate variability in the Aral Sea basin (Central Asia) during the Late Holocene based on vegetation changes. *Quat Res* 67:357–370.
66. Griggs C, DeGaetano A, Kuniholm P, Newton M (2007) A regional high-frequency reconstruction of May-June precipitation in the north Aegean from oak tree rings, A.D. 1089-1989. *Int J Climatol* 27:1075–1089.
67. Velud C (1987) Plan of land and agrarian structures in Syrian Jazira in the first half of the twentieth century. Territorial and Agrarian Structures in the Syrian Jazira in the First Half of the Twentieth Century (French) (Maison de l'Orient, Collection Etudes sur le Monde Arabe no. 2, Lyon), pp 161–194.
68. O'Brien R (2000) *Gertrude Bell, the Arabian Diaries 1913–1914* (Syracuse Univ Press, Syracuse).
69. Velud C (1997) French policy regarding tribes and steppe areas in Syria: The example of the Jazira. *Steppe d'Arabies, États, Pasteurs, Agriculteurs et Commerçants: Le Devenir des Zones Sèches*, eds Bocco R, Jaubert RF, Métral F (Presses universitaires de France, Paris), pp 61–86.
70. Reimer PJ, et al. (2009) IntCal09 and Marine09 radiocarbon age calibration curves, 0–50,000 years cal BP. *Radiocarbon* 51:1111–1150.
71. Bronk-Ramsey C (2009) Bayesian analysis of radiocarbon dates. *Radiocarbon* 51: 337–360.
72. Prentice IC, Guiot J, Huntley B, Jolly D, Cheddadi R (1996) Reconstructing biomes from palaeoecological data: A general method and its application to European pollen data at 0 and 6 ka. *Clim Dyn* 12:185–194.
73. Tarasov PE, et al. (1998) A method to determine warm and cool steppe biomes from pollen data; application to the Mediterranean and Kazakhstan regions. *J Quaternary Sci* 13:335–344.